ELSEVIER

Journal of Nuclear Materials 313–316 (2003) 976–979

journal of nuclear materials

www.elsevier.com/locate/jnucmat

Plasma–wall interactions and radial electric fields in the reversed field pinch RFX

L. Carraro, M.E. Puiatti, F. Sattin, P. Scarin, M. Spolaore, M. Valisa *, B. Zaniol, P. Zanca

Consorzio RFX, Associazione Euratom-ENEA sulla Fusione, Corso Stati Uniti 4, Padova I-35127, Italy

Abstract

The radial electric field E_r at the edge of the RFX plasma changes sign, from negative (inward) to positive, when an $m = 0$ perturbation is externally applied. Similar behaviour had been previously observed in presence of wall locked ($m = 1$) modes, whereby the much stronger plasma–wall interaction made data interpretation more complex. The findings are compatible with the presence of an $m = 0$, $n = 1$ magnetic island. While in ordinary situations the edge losses of RFX are interpreted as dominated by finite Larmor radius ion effects, inside the island associated with the external perturbation the diffusion of the electrons is enhanced and exceeds the ion loss flux, thus reversing E_r.
© 2003 Elsevier Science B.V. All rights reserved.

PACS: 52.40.H; 52.25.F
Keywords: Plasma wall interactions; Radial electric fields

1. Introduction

It is quite generally recognised that the $E \times B$ sheared flow mitigates turbulence and transport in magnetically confined plasmas [1]. A strong radial electric field (E_r) gradient of the order of 10^5 Vm^{-2} has been measured by independent means at the edge of the RFX reversed field pinch (RFP) experiment [2,3], in the region that features large pressure gradients. The measured E_r (inward at the wall) has a minimum at about 10 Larmor radii inside the last closed flux surface (LCFS) and then becomes positive further into the plasma where the magnetic field is stochastic [3]. Such a structure has been modelled by considering finite Larmor radius (FLR) induced ion losses as the dominant mechanism [4,5]. It has been observed that in the region of the first wall where the natural phase locking of several magnetohydrodynamic (MHD) modes deforms the plasma surface and causes strong plasma–wall interaction (PWI), the radial electric field reverses its sign: from negative (inward directed) to positive [6].

This paper presents analogous evidences of E_r reversal in RFX in presence of an externally induced ($m = 0$, $n = 1$) perturbation, which is used to force the rotation of mode locking [7], with the aim of mitigating its effects on the wall. The analysis of the $m = 0$ structure offers some advantages, in particular the lesser intensity of the PWI when the mode locking is not rotating. In the following the observed phenomenology is presented and the possible causes of the radial electric field inversion is discussed.

2. RFX experiment and experimental set up

RFX is a large RFP ($a = 0.46$ m, $R = 2$ m), a toroidal device in which by ohmic heating the plasma reaches electron temperatures T_e between 150 and 400 eV, with electron densities n_e in the range $0.1–1 \times 10^{20}$ m^{-3}, at plasma currents of 0.3–1.2 MA. In ordinary regimes the energy confinement time is of the order of 1 ms and a

* Corresponding author. Tel.: +39-49 829 5031; fax: +39-49 870 0718.
E-mail address: valisa@igi.pd.cnr.it (M. Valisa).

0022-3115/03/$ - see front matter © 2003 Elsevier Science B.V. All rights reserved.
PII: S0022-3115(02)01423-X

large ohmic input power (20–80 MW) is required to heat the plasma. The pulse duration is of the order of 150 ms. The topology of the RFP [8] features a reversal of the toroidal magnetic field typically at a normalised radius $r/a \sim 0.85$. Inside the reversal surface a number of resistive MHD $m = 1$ modes provide the dynamo electric field that sustains the configuration. This mechanism can produce either a state of field line multihelicity or a much more ordered quasi-single-helicity state [9].

The radial electric field at the edge has been diagnosed in two ways. By means of an insertable array of Langmuir probes radially aligned and 8 mm spaced, each measuring simultaneously the plasma floating potential V_f [10] – at the toroidal angle $\phi = 217°30'$ (Fig. 1). E_r is then deduced as $-\nabla_r V_f$, taking into account that $\nabla_r T_e \ll \nabla_r V_f$ in the RFX edge [10]. In the second approach, the Doppler shift of impurity emission lines [3] yields the toroidal flow of the impurities, in our case C III ($\lambda = 229.7$ nm), by using two opposite lines of sight tangent to the plasma centre, from two windows located on the equatorial plane 90° apart, at 142°30′ and 232°30′ respectively (Fig. 1). The result is therefore an average flow over two regions separated by 90°. Simultaneous measurement of the poloidal flow from two opposite vertical chords with an impact parameter of ~0.7 are also available at $\phi = 172°30'$. E_r results from the simplified (i.e., neglecting stress terms) radial momentum balance equation $E_r = (n_i Z_i e)^{-1}(\nabla p_i)_r(\boldsymbol{v}_i \times \boldsymbol{B})_r$, where the subscript i refers to the specific ion and E_r is the same for all the species. The diamagnetic term is assumed to be negligible for the low charge ions [3], due to the opposite and similar slopes of their radial distribution and considering $\nabla_r T_i$ to be negligible in the RFX edge.

3. Topology of plasma–wall interaction

In RFX, graphite tiles cover the vacuum vessel almost completely, without limiters. However, several $m = 1$ tearing modes locked in phase distort the plasma surface by several centimetres, so that the PWI is concentrated in helically shaped localised areas [11]. The addition of an external, toroidally rotating $m = 0$ radial magnetic field has been successful in dragging the locked mode structure around the torus, thus mitigating the effect of the localised PWI [11]. Fig. 2 shows the toroidal distribution of the $m = 0$, $n = 1$ magnetic field perturbation at a given time, obtained by reducing the voltage in six contiguous sections out of the 12 of the toroidal coil system. The positive value corresponds to a decrease of the reversed magnetic field at the wall. The propagation speed ranges from 250 to 500 m/s (i.e., ~100–200 rad/s). The typical applied error field is ~30 mT, corresponding to 50% of the toroidal field at the wall.

According to a non-axisymmetric reconstruction method that takes into account both $m = 1$ and $m = 0$ modes and is based on the B_ϕ pick-up coil data [12] the perturbation produces an outward displacement of the last magnetic surface of up to ~3 cm.

In the following we concentrate on those discharges in which the mode locking structure is not rotating (the amplitude of the $m = 0$ mode was too small) and the locked mode bulge is far from the diagnostic sections, so that the effect of the external rotating perturbation can be isolated.

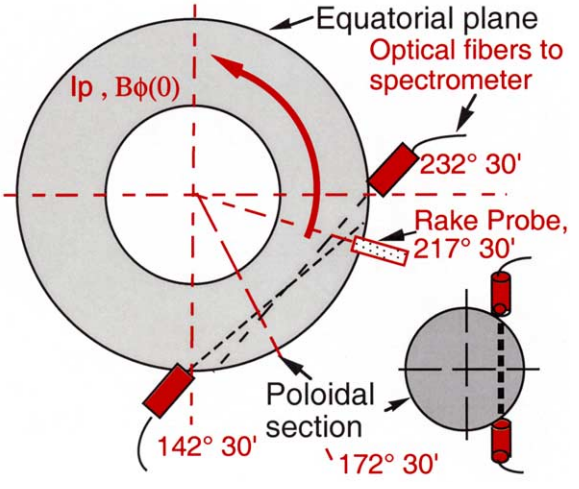

Fig. 1. Schematic of the experimental set up, showing the position of the optics for Doppler measurements and of the electrostatic probe.

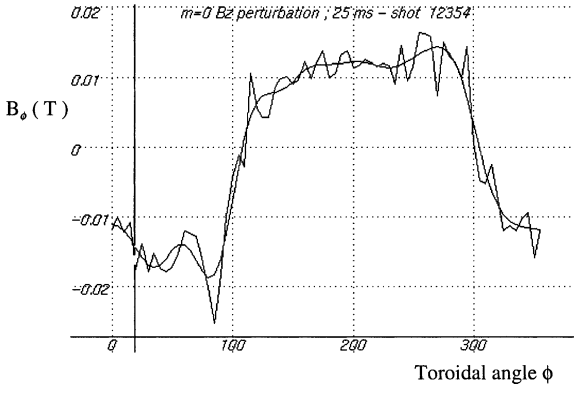

Fig. 2. Toroidal distribution of the $m = 0$ perturbation at 25 ms. A smoothing curve has been added to the discrete values reconstructed from the raw data of the toroidal array of B_ϕ coils. Positive values correspond to the region where the external perturbation is applied. The large oscillations at low ϕ are the signature of the $m = 0$ high n modes associated to the modes locked at the wall.

4. Radial electric field and plasma–wall interaction

C III emits in the outer 3–4 cm near the wall and is therefore sensitive to the edge variations of E_r. We assume that the CIII emission region does not change when the external perturbation is applied. This assumption is adequately substantiated by the measurements of a thermal He beam system [13] revealing, during the $m = 0$ perturbation phase, n_e increasing from 2×10^{19} to 4×10^{19} m^{-3} and T_e decreasing from 40 to 20 eV. Fig. 3 shows an example of both poloidal and toroidal CIII flow velocities as a function of time, together with the position of the centre of the rotating $m = 0$ perturbation. The toroidal velocity clearly decreases (in absolute value) and eventually changes sign as the perturbation, approximately 180° wide, approaches the region where the flow measurement is carried out (i.e., the region between 142°30′ and 232°30′ indicated in Fig. 3 by the two horizontal lines). The poloidal velocity, which is typically less than the toroidal one, changes also. The estimated error bar on the flow measurement is of the order of $+/-1$ km/s. Taking into account both toroidal and poloidal velocities E_r is calculated to change from −3 kV/m in the unperturbed situation to 1 kV/m when the $m = 0$ perturbation is in front of the diagnostic section. The evolution of the flow velocity indicates that the transition of E_r from negative to positive is relatively sharp. This behaviour is better evidenced by the poloidal velocity, which is measured in one toroidal location ($\phi = 172°30'$): when the front of the perturbation reaches the diagnostic section a transition in the poloidal velocity occurs in less than 2 ms. In addition, the poloidal velocity shows a different slope in time in correspondence of, respectively, the front and the bottom of the perturbation; this can be the signature of an asymmetry in the perturbation structure.

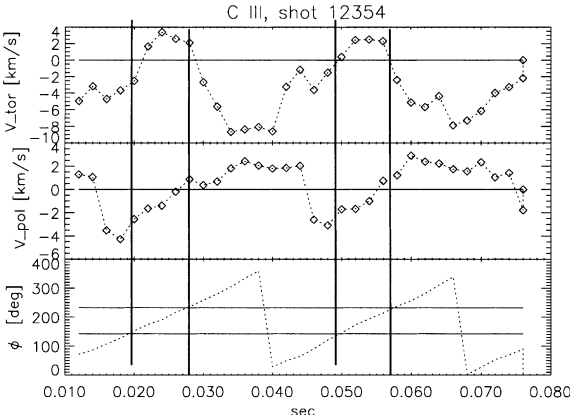

Fig. 3. Toroidal (top) and poloidal (middle) flow velocity of CIII vs. time and toroidal position of the centre of the external perturbation (bottom). In the bottom plot the horizontal stripe between 142° and 232° is the region where the Doppler measurement is carried out. Vertical stripes indicate when the measurement region is completely inside the perturbation pattern (approximately ±90° around the peturbation centre) in which case CIII flow clearly reverses its direction.

Floating potential data are available for shots at lower plasma current ($I_p = 300$ kA). Fig. 4 shows the evolution of the profile of E_r according to the probe data. The transition from negative to positive E_r occurs as soon as the external perturbation reaches the diagnostic section and E_r remains positive as long as the perturbation is present.

5. Discussion and conclusions

As mentioned above the radial profile of the electric field in absence of an external perturbation has been modeled in [4,5] considering the FLR ion losses as the

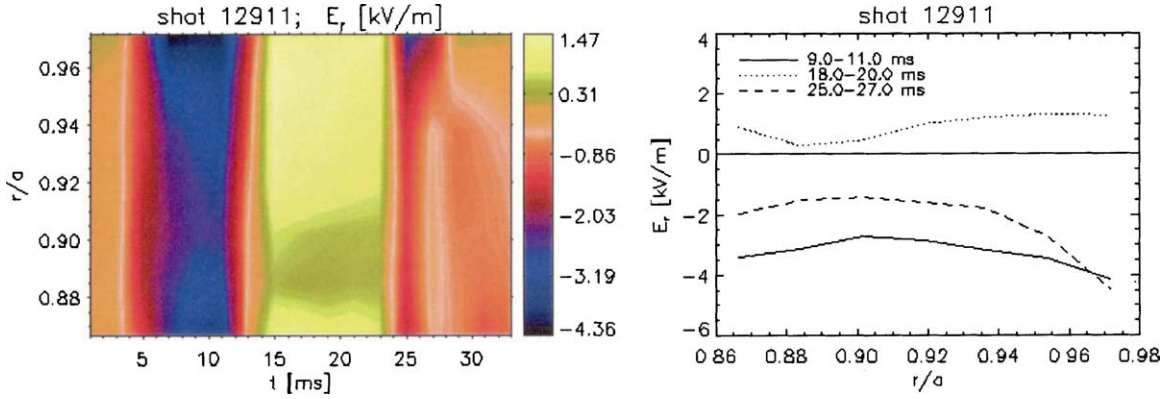

Fig. 4. Left: radial electric field profiles vs. time as measured by an array of seven eletcrostatic probes. The probes intercept the rotating $m = 0$ perturbation between 12 and 25 ms. Right: time averages of E_r profiles vs. normalised minor radius at three intervals as indicated in the plot. When the perturbation is present E_r reverses its sign.

crucial process. In the model, the return current balancing momentum and charge lost through the ions provides the momentum for accelerating the plasma in a direction normal to the local magnetic field. In the same model it was shown that dissipative terms as for example charge exchange with neutrals deepen the radial electric field to more negative values [5] and a viscous term would act in the same way. Therefore dissipative terms, which are indeed enhanced by the induced $m = 0$ perturbation, cannot explain the reversal of the electric field sign.

One possible cause for the change of the dominant charge loss mechanism is the presence of a radial magnetic field B_r. The field lines intercepting the wall would enhance the parallel electron losses up to overcoming the ion ones thus reversing the sign of the retarding field. However, as shown by Fig. 2, at $\phi \sim 180°$, corresponding to the centre of the perturbed region, the toroidal derivative value of the $m = 0$ perturbation is very low and similar to that at $\phi \sim 0°$, where no perturbation is applied. So, being proportional to the toroidal derivative of the toroidal magnetic field [14], B_r is negligible in both regions, while E_r is opposite. Therefore a radial magnetic field does not seem to be a convincing explanation for the observed behaviour of E_r.

Another, more convincing process that could explain the reversal of E_r at the edge is an enhancement of the electron losses associated to a high level of magnetic perturbation. In ordinary situations, corresponding in our context to an unperturbed external region, the edge particle flux is mainly driven by electrostatic fluctuations [15]. When an external perturbation $m = 0$, $n = 1$ is applied, due to the breaking of the magnetic surfaces a magnetic island is produced at the reversal surface ($r/a \sim 0.85$), with its O-point located in correspondence of the maximum of the external perturbation. The half radial extension of the island in a typical RFX discharge is calculated to be about 7 cm and the perturbation of the magnetic flux surface can indeed reach the wall. Due to its poloidal symmetry the $m = 0$ island is difficult to destroy [16]. When the amplitude of the $m = 0$ mode is relatively high, the region inside the island is characterised by a high diffusion rate; a situation in which the high mobility of the electrons along field lines dominate the losses. This behaviour is amplified when there is a non-linear coupling with internal $m = 1$ high n modes of relevant amplitude.

Moreover, the observed toroidal asymmetry of the perturbation structure may be explained as an asymmetry of the magnetic island produced by the presence of in phase higher n harmonic components. A deformation of the magnetic island may also be favoured by the viscous force induced by the plasma sheared flow associated with the phase gradient of the magnetic perturbation across the magnetic island [17].

The picture of $m = 0$ magnetic island could also explain the reversal of E_r found in the region where the external $m = 0$, $n = 1$ to 16 modes naturally lock in phase together with several internally resonating $m = 1$ modes. From a magnetic flux-surfaces computation (where the boundary conditions are given by the perturbed toroidal field measured at the shell) it appears a magnetic island whose width is $\sim$7 cm.

Finally we observe that the behaviour of E_r at the edge of RFX when applying an external perturbation has analogies with the results at the edge of Tokamak experiments with ergodic magnetic limiter (EML) configurations, where the same change of the E_r direction from negative to positive was found just inside the LCFS moving from limiter to EML configurations [18].

Acknowledgements

Clarifying discussions with R. Bartiromo, S. Cappello, F. D'Angelo, D. Escande, R. Paccagnella and S. Ortolani are kindly acknowledged.

References

[1] K. Burrell, Phys. Plasmas 4 (1997) 1499.
[2] V. Antoni, D. Desideri, E. Martines, et al., Phys. Rev. Lett. 79 (1997) 4814.
[3] L. Carraro, M.E. Puiatti, F. Sattin, et al., Plasma Phys. Control. Fusion 40 (1998) 1021.
[4] R. Bartiromo, Phys. Plasmas 5 (1998) 3342.
[5] V. Antoni, R. Bartiromo, L. Carraro, et al., Czechoslovak, J. Phys. 50 (12) (2000) 1387.
[6] M.E. Puiatti, L. Tramontin, V. Antoni, et al., J. Nucl. Mater. 290–293 (2001) 696.
[7] R. Bartiromo, T. Bolzonella, A. Buffa, et al., Phys. Rev. Lett. 83 (1999) 1779.
[8] S. Ortolani, D.D. Schnack, Magnetohydrodynamics of Plasma Relaxation, World Scientific, Singapore, 1993.
[9] E.F. Escande, P. Martin, S. Ortolani, et al., Phys. Rev. Lett. 85 (2000) 1662.
[10] V. Antoni, E. Martines, D. Desideri, et al., Plasma Phys. Control. Fusion 42 (2000) 83.
[11] M. Valisa, R. Bartiromo, et al., J. Nucl. Mater. 290–293 (2001) 980.
[12] P. Zanca, S. Martini, Plasma. Phys. Contr. Fusion 43 (2001) 121.
[13] L. Carraro, G. De Pol, M.E. Puiatti, et al., Plasma Phys. Control. Fusion 42 (2000) 1.
[14] P. Zanca, E. Martines, T. Bolzonella, et al., Phys. Plasmas 8 (2001) 516.
[15] V. Antoni, R. Cavazzana, D. Desideri, et al., Phys. Rev. Lett. 80 (1998) 4185.
[16] F. D'Angelo, R. Paccagnella, Phys. Plasmas 3 (1996) 2353.
[17] C. Ren, M.S. Chu, J.D. Callen, Phys. Plasmas 6 (1999) 1203.
[18] Ph. Ghendrih, A. Grosman, H. Capes, Plasma Phys. Control. Fusion 38 (1996) 1653.